American Mineralogist, Volume 75, pages 1238–1248, 1990

Infrared spectra of GeO_2 with the rutile structure and prediction of inactive modes for isostructural compounds

ANNE M. HOFMEISTER
Department of Geology, University of California, Davis, California 95616, U.S.A.

JOANNE HORIGAN
University of Nevada at Reno, Reno, Nevada 89557, U.S.A.

JULIE M. CAMPBELL
San Diego State University, San Diego, California 92101, U.S.A.

ABSTRACT

A thin-film infrared (IR) spectrum of very fine-grained synthetic GeO_2 having the rutile structure shows all four bands expected from symmetry analysis. Through comparison of these data to previous contradictory reflection data (Kahan et al., 1971; Roessler and Albers, 1972), longitudinal optic (LO) and transverse optic (TO) positions were accurately established for all bands in both the E_u and A_{2u} polarizations. Examination of the available vibrational data on 11 rutile structure compounds shows that Raman frequencies for each type of anion smoothly decrease as a function of both cell volume and cation-anion bond length. IR frequencies follow similar trends regardless of type of anion present, except for SnO_2, which is probably caused by the much heavier mass of Sn, or a different percentage of covalent or ionic character in its bonding from that in other rutile structure compounds. The consistency of the trends, along with two measurements and one calculated value for inactive modes in TiO_2, allows reasonable estimates to be made for $2B_{1u}$ and A_{2g} in all the other rutile types. Our estimates appear to be at least as accurate (± 50 cm^{-1}) as recent lattice dynamic calculations (e.g., Maroni, 1988). Comparisons of vibrational frequencies made using the Gordy formulation for the force constant produced the same type of smooth, nonlinear trends as did the dependence of frequency on cell volume, which suggests that the force constants are not a simple relationship of reduced mass, bond length, and electronegativity or valance. We suggest that for solids, additional factors affecting the value of vibrational frequencies are relative bond compressibilities and bond strengths.

INTRODUCTION

Stishovite (SiO_2 with the rutile structure) is important in the mantle, partly because of its wide stability range. Experimental difficulties encountered in determining its physical properties over pertinent mantle pressures make study by analogues tempting, if not necessary. Moreover, the sixfold coordination of Si in stishovite as opposed to fourfold coordination of Si in the other SiO_2 polymorphs limits their usefulness in predicting stishovite's macroscopic properties. Germanates are the first choice as an analogue to silicates owing to similarities in bonding, although comparison to other rutile-structure compounds is helpful.

This study reports thin-film infrared frequencies for GeO_2 isostructural with rutile. Comparison of these data to previous infrared (IR) reflectance spectra (Kahan et al., 1971; Roessler and Albers, 1972) resolves the discrepancy between the two prior data sets. Comparisons of the spectra of GeO_2 and ten other rutile compounds are made through the dependences of vibrational frequencies on cell volume and bond length. The trends are sufficiently consistent to constrain positions of the inactive bands. These estimates may be more accurate than recent lattice dynamic calculations of Maroni (1988). Reasonably constrained values for the inactive modes are essential for construction of interatomic potentials and in determining thermodynamic properties. Using these estimates, bulk moduli are accurately calculated using the model of Hofmeister (in preparation). A companion paper (in preparation) will show how heat capacity and entropy can be accurately calculated for stishovite, rutile, and GeO_2.

EXPERIMENTAL

GeO_2 was synthesized with the rutile structure in a solid-media high-pressure apparatus similar to that described by Boyd and England (1960). Starting material was high-purity GeO_2 (less than 10^{-5} wt% impurities) sealed in a Pt container with a drop of H_2O added to facilitate production of large crystals. Temperature was measured with a Pt90-Rh10 thermocouple. Pressures were

0003–004X/90/1112–1238$02.00

calibrated to within 1 kbar by the phase transitions quartz-coesite, calcite-aragonite, and albite-jadeite. Two syntheses were attempted at 10 kbar (one charge was held entirely at 900 °C for 48 h; the second charge was first melted at 1400 °C for 1 h, after which the temperature was dropped 1°/min to 1200 °C, followed by annealing for 24 h). Because both attempts yielded fine-grained powders of about 10-μm grain size and because further annealing of the samples did not induce enough growth to produce crystals of sufficient size for reflection spectroscopy, we made no further attempts to synthesize GeO_2 with the rutile structure.

IR spectra were obtained using a Nicolet 7199 optical bench and a Nicolet 1280 data processor. Far-IR absorption spectra were obtained at a resolution of 4 cm^{-1} from about 500 to 70 cm^{-1} using a liquid-He cooled Si-bolometer (Infrared Laboratories, Tucson, Arizona) from a powdered sample compressed into a thin film (ca. ½–2 μm) by a diamond-anvil cell. Pressure was released prior to measurement. Mid-IR spectra were similarly obtained at a resolution of 1 cm^{-1} at wavenumbers above 400 cm^{-1} using a HgCdTe detector coded with liquid N_2. The resulting far-IR data were scaled to match the mid-IR throughout the region of overlap before the data from the two files were merged.

Vibrational spectroscopy

The number of zone-center vibrations for the rutile-type structure (space group $P4_2/nmm$ or D_{4h}^{14} with $Z = 2$) is predicted by symmetry as $A_{1g}(R) + A_{2g} + B_{1g}(R) + B_{2g}(R) + E_g(R) + 2B_{1u} + A_{2u}(IR) + 3E_u(IR)$, where R indicates Raman active bands and IR indicates infrared active bands. However, the type of motion cannot be derived from factor-group analysis because of lack of isolated structural units. Analysis of the dynamical matrix allows description of the modes at zone center in terms of relative displacement (Dayal, 1950). Pictures of the modes are found in Traylor et al. (1971); an abbreviated description is given in Table 1.

In rutile, metal ions are at centrosymmetric sites and thus are not displaced in the gerade modes. As a result, the Raman spectra of all rutile-type compounds with the same kind of anion are expected to be similar, such that bands will shift with changes in lattice constant or bond length, as well as with other factors likely to influence force constants, such as electronegativity, valance, and anion mass. In contrast, the ungerade vibrations should depend strongly on cation mass, in addition to the factors likely to affect Raman frequencies. The dependencies of the IR and Raman modes on the above factors will be discussed in a later section.

Previous IR and Raman data on rutile structure compounds

Study of rutile (TiO_2) by infrared reflection spectroscopy (Eagles, 1964), Raman scattering (Porto et al., 1967), and inelastic neutron scattering (Traylor et al., 1971) has determined all but one of the zone center vibrational modes. The energy of the missing A_{2g} mode has been calculated through lattice dynamics by Katiyar and Krishnan (1967); its value is presumed accurate because of the excellent agreement obtained for the other gerade species and fair-to-good agreement for the ungerade species. Rutile itself is problematic in that the presence of the many weak secondary features in its Raman spectra suggests distortion from the ideal structure (Hara and Nicol, 1979).

For stishovite (SiO_2), IR reflectance, thin-film absorption (Hofmeister et al., 1990a), and Raman scattering (Hemley et al., 1986) have determined frequencies for all of the active modes. For cassiterite (SnO_2), IR reflectance (Katiyar et al., 1971) and Raman scattering measurements (Peercy and Morosin, 1973) have provided frequencies for all of the active modes.

Raman spectra of GeO_2 show four bands (Sharma et al., 1979) with intensity and position patterns similar to the other rutile structure compounds. However, the IR reflectance spectra of Kahan et al. (1971) show five bands in E_u polarization , compared to three mandated by symmetry, and a doublet in A_{2u} where a singlet should be.

Table 1. Rutile structure modes

Type	Description	GeO_2 LO-TO	SiO_2 LO-TO	TiO_2 LO-TO	SnO_2 LO-TO (f)	RuO_2 LO-TO (l)	MgF_2 LO-TO	NiF_2 LO-TO (k)	ZnF_2 LO-TO	CoF_2 LO-TO	FeF_2 powder	MnF_2 LO-TO (i)
$B_{1u}(2)$	stretch			113 d								
B_{1g}	rotation	166 g	231 b	142 d	123 m	97	92 i		70 i		73 i	61
$E_u(3)$	stretch	350–300 a	565–470 c	374–189 d	276–244 f		303–247 j	250–228	227–173 j	233–196	200 k	
$B_{1u}(1)$	bend			406 d								
$E_u(2)$	stretch	470–350 a	700–580 c	428–388 e	366–293 f		415–410 j	300–286	264–244 j	295–268	320 k	
E_g	rotation	420 g	589 b	445 d	476 m	528	295 i		253 i		257 i	247
A_{2g}	bend			573 h								
A_{1g}	stretch	700 g	753 b	610 d	637 m	646	410 i		350 i		340 i	341
A_{2u}	stretch	755–445 a	960–675 c	811–173 d	705–477 f		625–399 j	538–370	488–294 j	500–340	440 k	
$E_u(1)$	stretch	815–635 a	1020–820 c	841–494 d	770–618 f		617–450 j	550–440	498–380 j	510–412	480 k	
B_{2g}	stretch	874 g	967 b	824 d	781 m	716	515 i		522 i		496 i	476

Note: a = Roessler and Albers (1972); lowest energy modes modified (see text), b = Hemley et al. (1986), c = Hofmeister et al. (1990a), d = Traylor et al. (1971), e = Eagles (1964), f = Katiyar et al. (1971), g = Sharma et al. (1979), h = Katiyar and Krishnan (1967), i = Porto et al. (1967), j = Barker (1964), k = Balkanski et al. (1966), l = Huang and Pollak (1982), m = Peercy and Morosin (1973).

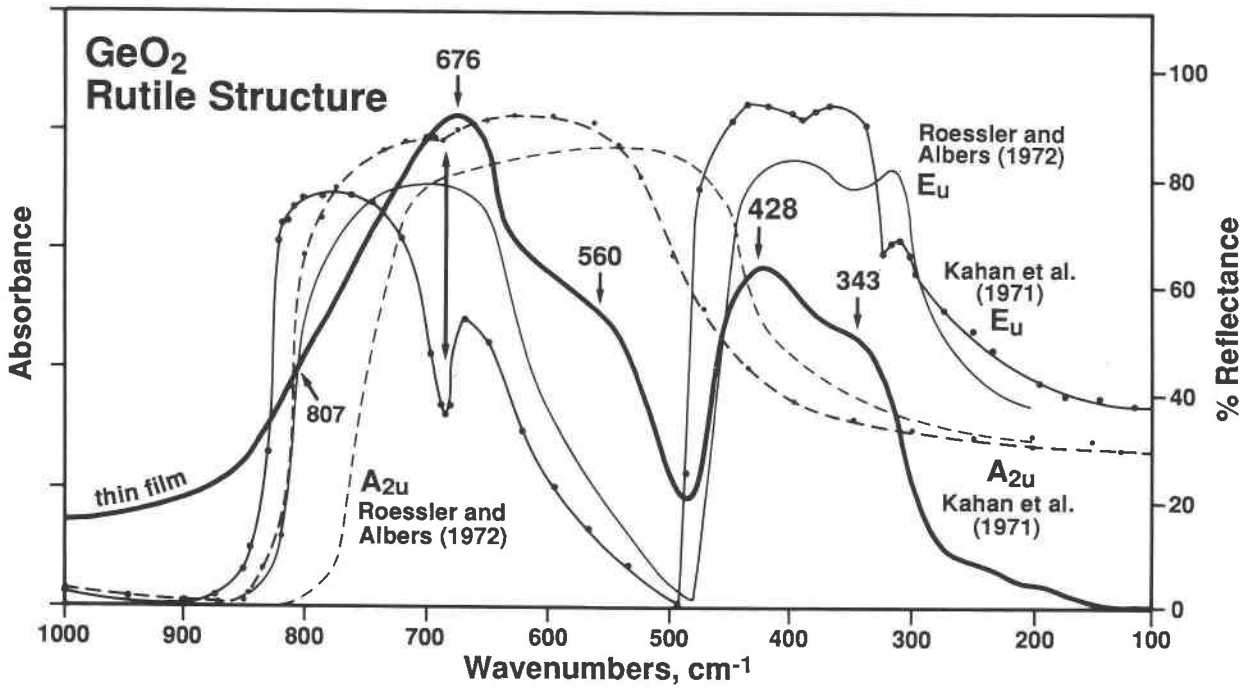

Fig. 1. Rutile-structure GeO_2 infrared spectra. Heavy solid line, merged IR absorbance spectrum with peak positions as indicated. Weak bumps near 200–300 cm^{-1} are attributed to absorbed H_2O. Light dashed line, E_u polarization (electric vector perpendicular to the c axis) and light dotted line, A_{2u} polarization (E parallel to c) of Roessler and Albers (1972). Light solid line with dots, E_u polarization reflectance and light dashed line, A_{2u} polarization of Kahan et al. (1971). Note that the doublet in E_u contains the two lowest energy thin-film peaks and that both E_u and A_{2u} contain a dip near 680 cm^{-1}.

Moreover, the intensity pattern is not like that of other oxides occurring in the rutile structure. We suspect that some degree of polarization mixing is present in these experiments, resulting in extra bands. Reflectance measurements for GeO_2 (Roessler and Albers, 1972) have the correct number of bands, but two bands were juxtaposed so that the authors found it necessary to artificially resolve them. The intensity pattern of Roessler and Albers (1972) strongly resembles that of stishovite and those of the other compounds isostructural with rutile.

IR reflectance (Barker, 1964) and Raman measurements (Porto et al., 1967) on MgF_2 and ZnF_2 revealed all active modes. The intensity patterns resemble those of the oxides, but the peaks occur at much lower frequencies and over a smaller range.

Single-crystal Raman data, but not IR, are available on RuO_2 (Huang and Pollak, 1982) and on FeF_2 and MnF_2 (Porto et al., 1967). Balkanski et al. (1966) measured powder IR data for FeF_2, and single-crystal IR reflectance data on CoF_2 and NiF_2, but no Raman data are available for these compounds.

New IR data on GeO_2: Reassessment of reflectance data

Figure 1 shows the presence of four strong-to-medium bands in the thin-film spectra, as is expected for the rutile structure. The intensity pattern of these four bands strongly resembles that of stishovite and the other rutile-type compounds (described in the previous section). The weakest band, at 560 cm^{-1}, belongs to the A_{2u} symmetry. The thin-film technique yields transverse optic (TO) positions for low intensity far-IR modes in olivine (Hofmeister et al., 1989) and garnet (Hofmeister et al., 1990b); although, for intense mid-IR modes, the positions are shifted toward the longitudinal optic (LO) component. For stishovite, the shifts are negligible to 20 cm^{-1} (Hofmeister et al., 1990a), but for SiO_2 the LO modes are well-resolved, as opposed to that for GeO_2, where they are not readily discernible (Fig. 1). The presence of LO modes in thin-film spectra is expected because of (1) finite film thickness (Berreman, 1963) and (2) oblique incidence of light on the sample caused by focusing through the diamond anvils. These two effects exacerbate each other. Therefore, the LO components that are expected in the GeO_2 thin-film IR spectrum must be merged with their TO counterparts. We attribute this departure in behavior from stishovite to smaller LO-TO splitting in GeO_2 than in SiO_2 (Table 1). Merging of the LO and TO components also explains the somewhat larger breadth of the GeO_2 thin-film peaks as compared to those in stishovite (Hofmeister et al., 1990a) and olivine (Hofmeister et al., 1989). The widths of Si-O peaks of stishovite or olivine (ca. 50–80 cm^{-1}) are altogether too large to result merely from use of diamond anvils and the finite film thickness. Thus, Si-O stretching peaks are intrinsically broad, so it is reasonable to expect that stretching modes of other oxides will have similarly large widths. The thin-film peaks of

GeO_2 appear to be 50–100 cm^{-1} higher than the TO frequencies derived from reflectance measurements. The above analysis is supported by the fact that the highest energy E_u band is shifted the least from the TO positions and shows a very weak shoulder near the LO component.

Comparison of the thin-film data on GeO_2 with the E_u reflectance spectrum of Roessler and Albers (1972) corroborates their inference that the intense band from about 330–500 cm^{-1} is a poorly resolved doublet. As an alternative to artificially resolving these two reflectance bands, we infer their position from comparison of the three data sets. Examination of the thin-film spectra suggests a lower limit of $E_u(3)$ LO as 343 cm^{-1} and an upper limit as 380 cm^{-1}. The spectrum of Kahan et al. (1971) better resolves $E_u(2)$ TO, with a position of 333 cm^{-1}; however, the TO component of $E_u(2)$ must be higher than that of the LO component of $E_u(1)$ or an LO/TO reversal occurs, as documented in quartz by Scott and Porto (1967) and in garnets (Hofmeister et al., 1990b). The appearance of the reflectance and absorption spectra of GeO_2 are not equivalent to spectra of quartz or garnet with demonstrable reversals; therefore the LO component of $E_u(2)$ must be higher than 343 cm^{-1}. A reasonable compromise for both peaks is 350 $\pm$ 10 cm^{-1} (Table 1), which is the position of minimum in the reflectance spectra of Roessler and Albers (1972).

Artifacts in the spectra of Kahan et al. (1971) can be explained as follows: The narrow weak band from 620 to 680 cm^{-1} in E_u results from a combination of the 300 and 350 cm^{-1} TO bands in E_u. The closeness of the $E_u(1)$ TO position at 635 cm^{-1} to the sum of the two lower energy TO bands in E_u is conducive to creating a resonance (intensity stealing), leading to a larger-than-normal intensity for the overtone and the appearance of extra bands in each of E_u and A_{2u}. The minimum in reflectance at 680 cm^{-1} in A_{2u}, which is 100 times weaker than the corresponding minimum in E_u, is obviously caused by polarization mixing. Similar polarization mixing also results in the higher LO position for A_{2u}. Such mixing was seen in SnO_2 by Katiyar et al. (1971). Lastly, the origin of the extra peak at 400–450 cm^{-1} in E_u is readily explained by the weak presence of the A_{2u} TO mode.

Comparison to other rutile structure compounds: Inferences on factors affecting mode frequencies

The existing IR and Raman data for five oxides and six fluorides provide a basis with which to test various factors that have been proposed to affect the values of the vibrational frequencies. We begin with simple tests of the relationship of frequency with cell volume or bond length, and then investigate formulas for force constants. Our motivation is not so much to evaluate the applicability of the various formulations, but to see if consistent, simple, trends exist that may be used either to predict missing modes for rutile compounds with partial spectroscopic data or to provide constraints on the values for the inactive modes for compounds with all active modes accounted for. Because of the greater importance of the latter as inputs for thermodynamic and elastic models, we have not separated the oxides from the fluorides in examining dependence of frequency on cell volume or bond lengths. Cell volume was chosen because linear dependencies upon it were found for silicate garnet frequencies (Hofmeister et al., 1990b). Bond length was chosen because it is known to play a role in the force constants (Batsanov and Derbeneva, 1969). Structural data for stishovite were taken from Hill et al. (1983). For all other compounds, data from Wyckoff (1965) were used.

Raman frequencies for compounds with the rutile structure and having the same anion follow parallel, decreasing trends with cell volume (Fig. 2a). Trends for the B_{1g}, B_{2g}, and A_{1g} symmetries are close to linear. Note that the trend of the lowest energy peak (B_{1g}) is much flatter and smoother than any of the others. This observation may be connected with B_{1g} motion being a pseudorotation (Dayal, 1950; Traylor et al., 1971), in that rotations are generally less dependent on cell size or any other parameters than are other bands, and the contribution to frequency from differences in cation mass is negligible compared to the mass of the six anions involved. This particular mode distorts the rutile structure toward the fluorite structure. Mode softening of B_{1g} has been observed for TiO_2 (Nicol and Fong, 1971; Samara and Peercy, 1973; Mammone et al., 1980), SnO_2 (Peercy and Morosin, 1973), and SiO_2 (Hemley, 1987).

The IR frequencies in compounds isostructural with rutile have a pattern that is similar to the Raman bands but not as consistent (Figs. 2b–2d). The general trend is a decrease in the LO or TO or average frequency with increasing cell volume, regardless of type of anion present. Exceptions are cassiterite, which has much higher frequencies than the trends, and TiO_2, which has two LO bands that are higher and one TO band that is considerably lower than the trends of the other compounds. The IR trends are not parallel, as observed for the Raman; instead, the zigzags in the pattern become less prominent as the energy of the mode decreases [i.e., the $E_u(3)$ trend is much flatter than the $E_u(1)$ trend].

The departure of data for cassiterite from the IR trends, but not the Raman trends, may be associated with its cation mass of 118.7 amu for Sn being nearly double that of the next heaviest cation (Ti at 72.59) and being nearly four times that of the lightest cation (Mg at 24.03), since the cation does not move in the Raman modes, whereas the cations vibrate in IR modes. Thus, the latter should strongly depend on cation mass. The difference cannot be attributed to large cell size, because compounds with the fluorite structure having even larger cells follow the same trends as the oxides with the rutile structure that have small cells. (Figs. 2b–2d). The existence of a very heavy mass in cassiterite could decouple the anion from the cation motions or perhaps require considerably different force constants. Another possibility is that the relative proportions of ionic, covalent, and metallic character for the Sn-O bond differ from proportions found in the other rutile structure compounds. For TiO_2, the dif-

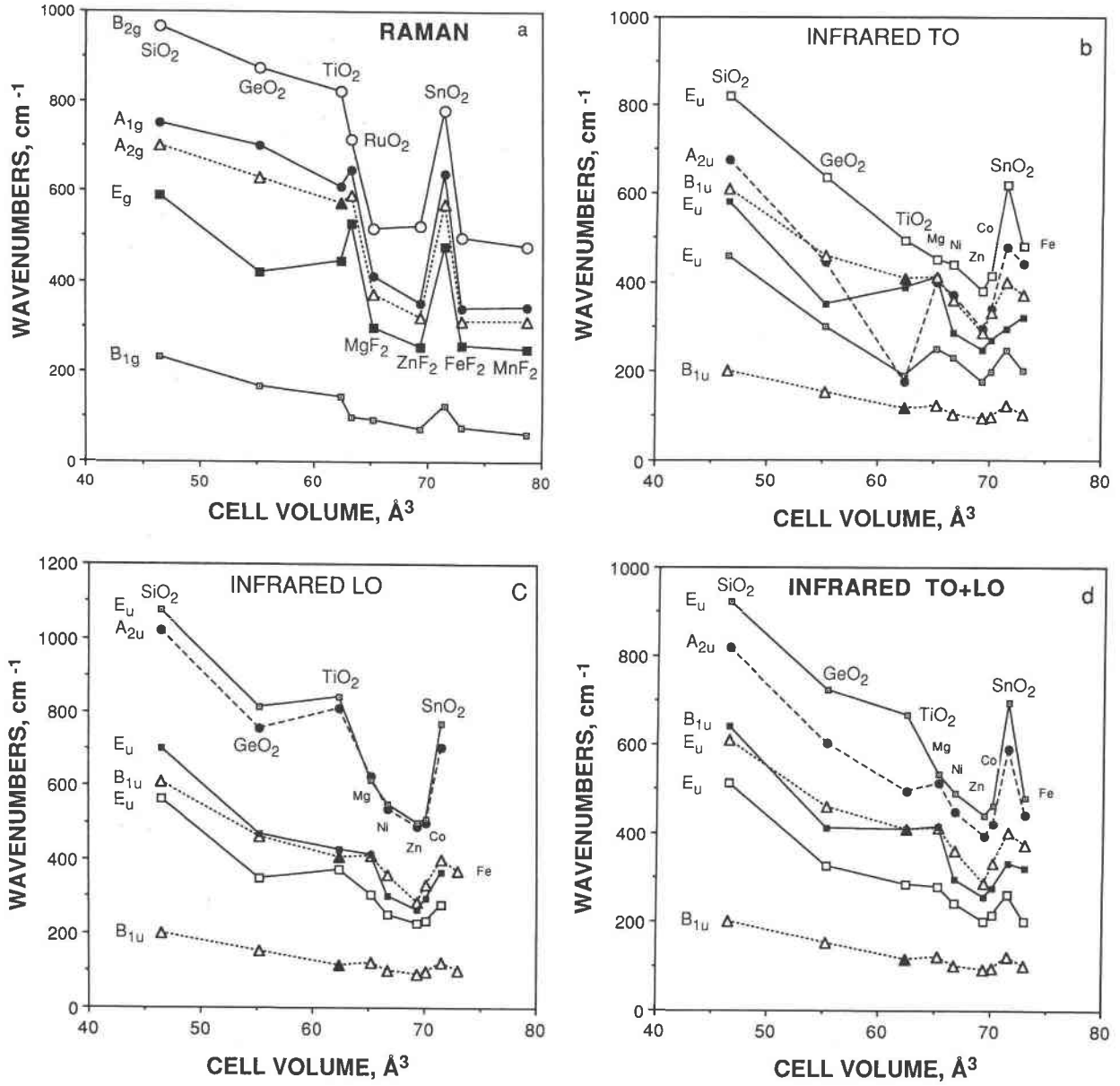

Fig. 2. Dependence of vibrational bands on cell volume in compounds isostructural with rutile. (**a**) Raman modes and the one gerade inactive mode (B_{1g}). (**b**) IR TO modes and the two ungerade inactive modes, B_{1u}. (**c**) IR LO modes and B_{1u}. (**d**) Average of the TO and LO infrared modes and B_{1u}. Lines are labeled according to symmetry. For the A_{2g} mode in TiO_2, frequencies were calculated from lattice dynamics: frequencies for the B_{1u} modes (filled triangles) were measured by Traylor et al. (1971). Inactive frequencies were estimated for all other compounds (see text). The Raman modes show a somewhat more consistent decreasing trend with frequency for the compounds with alike anions as cell volume increases, as is expected because the gerade modes do not involve the cation. When SnO_2 is excluded, the IR modes show a smooth and strongly decreasing frequency with volume, regardless of composition. Sources of data are in Tables 1 and 2 and in the section on previous vibration spectra.

ferences are highly likely related to this compound having a dielectric constant that is exceptionally high and temperature dependent, although a ferroelectric transformation is not observed; this contributes to the large polarizability and hence large LO-TO splitting of its IR modes. Raman modes are little affected by the polarizability, which explains the more consistent trends of frequency with cell volume (Fig. 2a).

The overall decrease of frequency with cell volume can be related to bond strengths or to force constants. As the

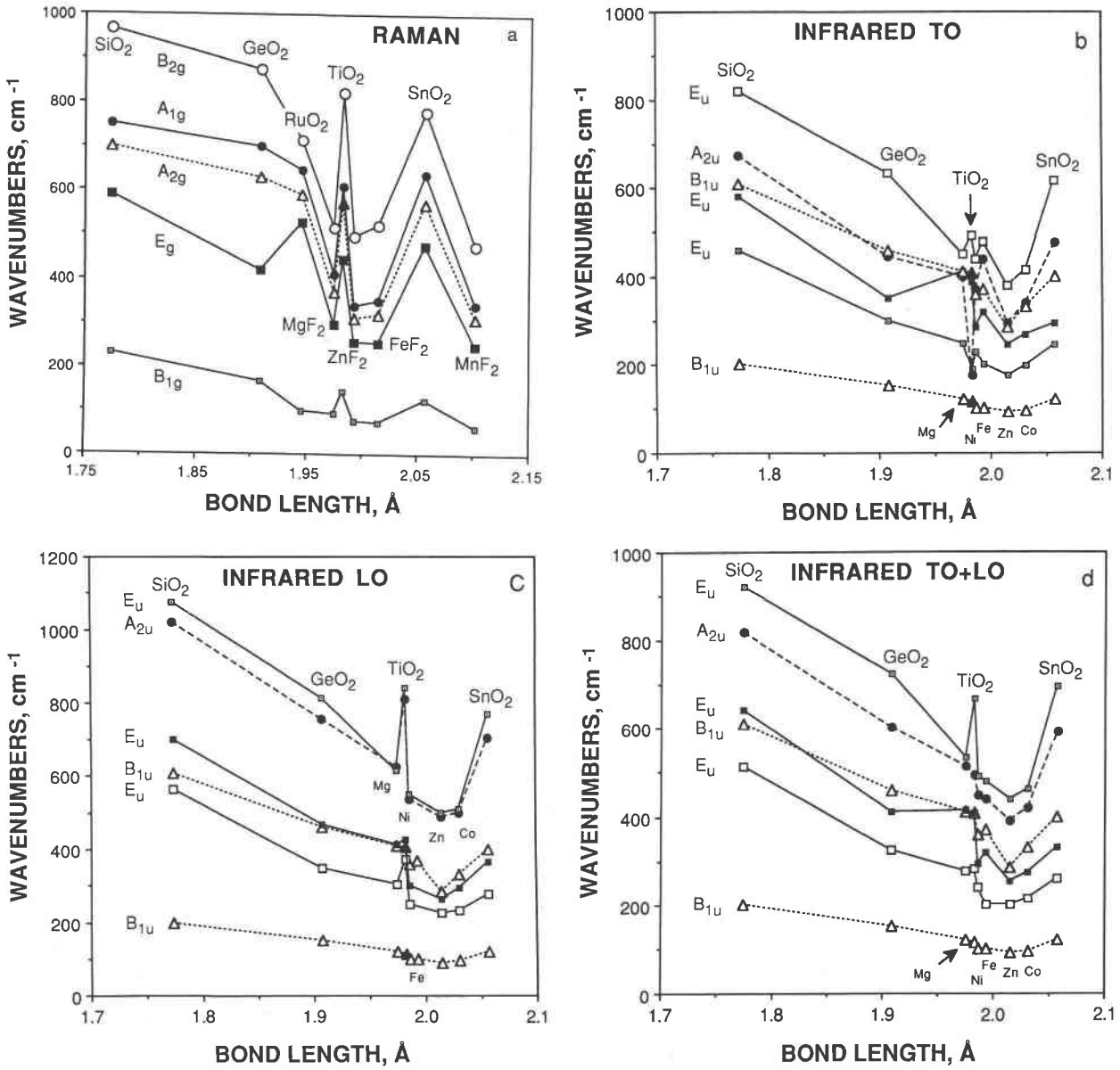

Fig. 3. Dependence of vibrational frequencies on cation-anion bond length. (**a**) Gerade modes. (**b**) IR TO modes and B_{1u}. (**c**) IR LO modes and B_{1u}. (**d**) Average of IR LO and TO modes and B_{1u}. See caption of Figure 2 for further details.

structure is pulled apart, the longer bonds are expected to be weaker, so frequency is lower. The analogy to a particle in a box may also be made. There is a secondary effect due to cation mass in that TiO_2 modes are lower than those of an average linear trend, whereas MgF_2 modes are slightly higher (Figs. 2b–2d). The existence of separate quasi-linear trends for the oxides and fluorides for the Raman modes but only one roughly monotonically decreasing trend for IR modes (Fig. 2d) can be accounted for by considering that only the anions participate in the Raman modes (two trends for two anions), whereas the IR modes are best described entirely as cation-anion stretching modes (one trend for the size of the box, that is modified by the masses of the ions).

Similar correlations are seen between the vibrational frequencies and cation-anion bond lengths for all observed modes (Fig. 3). For some of the modes, this type of plot yields more consistent behavior than the trends with cell volume. For others, the curves are more jagged, rather than smoother. Similar correlations should occur for frequency with cell volume and cation-anion bond length r because the two parameters are related:

$$r = 2^{1/2}au \qquad (1)$$

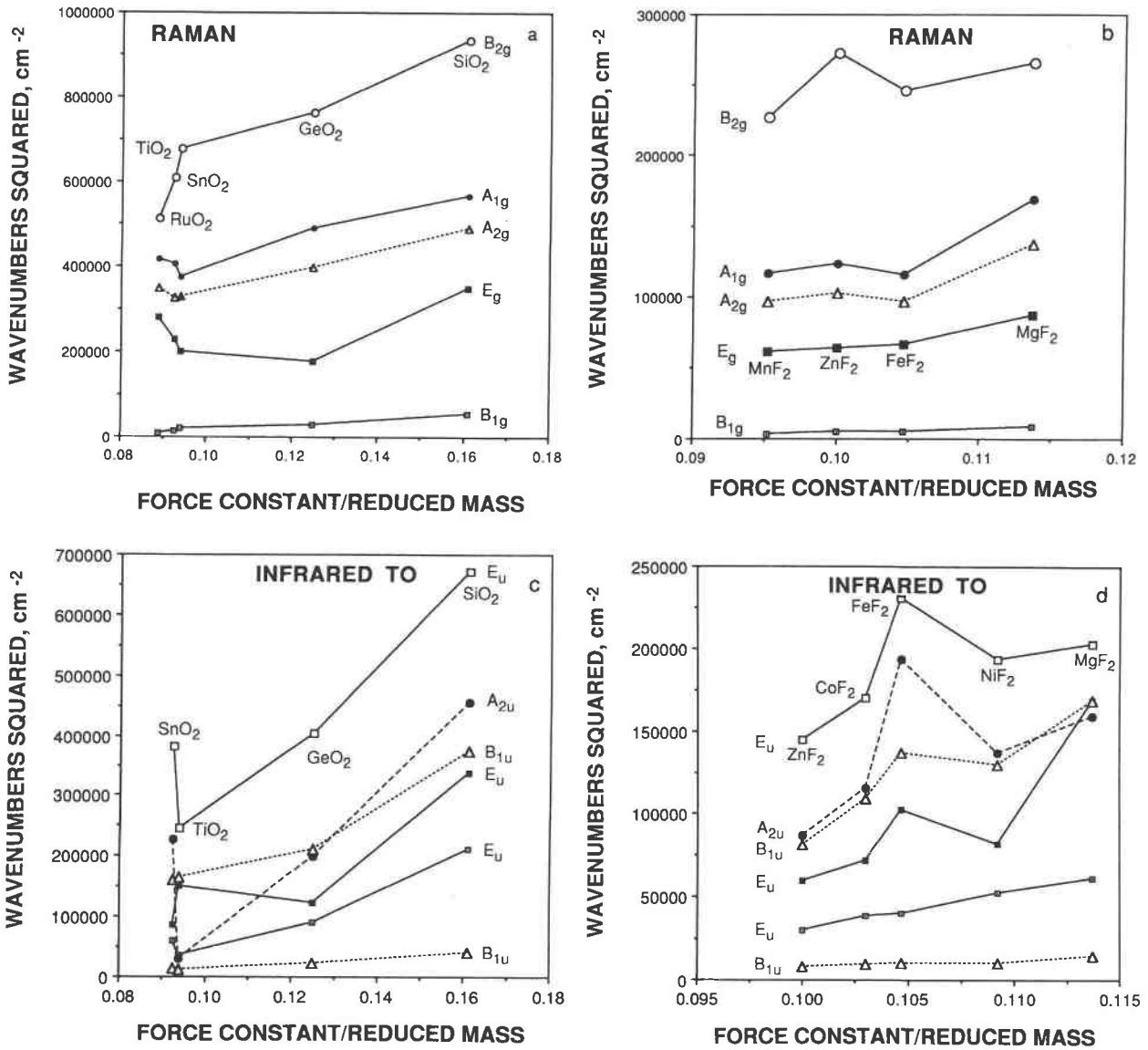

Fig. 4. Dependence of the square of the vibrational frequencies on force constant divided by reduced mass. (a) Gerade modes for the oxides. (b) Gerade modes for the fluorides. (c) Ungerade TO modes for the oxides. (d) Ungerade TO modes for the fluorides. Force constants were calculated from Equation 4. See caption of Figure 2 for further details.

where a is one of the lattice constants and u is the anion positional parameter.

A vibrational frequency can be related to a force constant k and the reduced mass μ through

$$\nu = (k/\mu)^{1/2}. \quad (2)$$

For covalent solids, Batsanov and Derbeneva (1969) used the Gordy formula to approximate k:

$$k = a(X_+X_-/r^2)^{3/4} + b, \quad (3)$$

where a and b are constants and X is the electronegativity of each of the two ions. If this relationship is correct for compounds with the rutile structure, then

$$\nu^2 \propto [(X_+X_-/r^2)^{3/4}]/\mu = k'/\mu, \quad (4)$$

where k' is the reduced force constant. The slopes and offsets may vary between the oxides and fluorides because of the different valencies of the constituent atoms. The reduced mass was calculated from the atomic masses of the cation and anion for each compound (this should be strictly correct for the ungerade modes, which are essentially cation-anion stretching motions, but is an approximation for the gerade modes). Electronegativities were taken from the scale of Little and Jones (1960). Figure 4

shows that ν^2 is not linearly dependent on k'/μ. In fact, the trends are slightly less smooth and regular than the plots of frequency vs. cell volume or bond length.

There is some question as to the correctness of using the reduced mass for the gerade modes in which the cation does not participate. If the reduced mass is entirely related to anions, then it is the same for all the fluorides or for all the oxides, and ν^2 should be linearly dependent on k'. Figure 5 clearly shows that this is not the case; in fact, the dependence of ν^2 on k' is considerably less regular than that of frequency on cell volume. It is apparent in comparing Figures 4 and 5 that cation mass plays a role in determining the frequencies of the gerade modes, even though the cations are not active participants in the atomic motion. This observation can be rationalized in that the motions of the anions stretch the cation-anion bond even though the cation is fixed in space. For example, B_{1g} is essentially a rotation of the XO_6 octahedron, so that the reduced mass must involve six anions but only one cation. Thus, the mass of the cation is pertinent to the Raman frequencies, but is not as strong an influence as that on the IR modes. The effect of force constants on the ungerade modes was also tested (Appendix Fig. 6[1]) and found to be poorly correlated. Also, simple, straightforward relationships do exist between ν^2 and reduced mass (Appendix Fig. 7[1]) but these are not inversely linear as Equation 2 would suggest.

Thus, force constants for modes in the rutile structure are clearly affected by factors such as mass, electronegativity, bond length, and cell volume. Obviously other important characteristics have been overlooked because the linear relationship implicit in Equation 4 was not seen. The assumptions that Batsanov and Derbeneva (1969) used to derive the force constant of Equation 3 originate in our understanding of chemical bonding of molecules in the gaseous state. Solids are not equivalent. Of utmost importance is the fact that the radical does not vibrate in isolation. As shown theoretically by Brout (1959), the sum of the vibrational frequencies for an ionic solid is directly proportional to the bulk modulus of the solid. Brout's arguments can be extended to covalent solids (Mitra and Marshall, 1964), and extensions of his formula to a variety of mineral structures, including rutile, yield fairly accurate predictions of bulk moduli from vibrational frequencies (Hofmeister, in preparation). These relationships lead us to infer that one missing factor in current formulations of force constants is the compressibility of the cation-anion bond. Partial evidence for this lies in (1) the consistent relationship between cell volume and frequencies, in that the compressibility of the bond will be determined by how tightly the crystal structure is packed; (2) the close relationships of bulk moduli of the crystal to polyhedral bulk moduli and polyhedral linkages

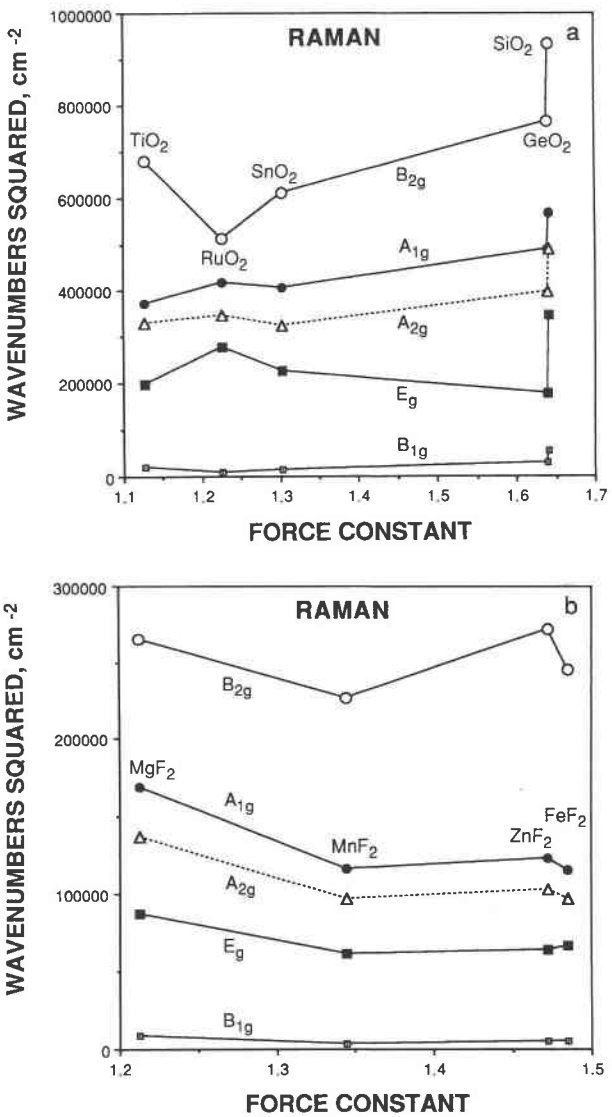

Fig. 5. Dependence of the square of the vibrational frequency of the gerade modes from rutile structure compounds on force constant. (a) Oxides. (b) Fluorides. Force constants were calculated from Equation 4. See caption of Figure 2 for further details.

(Hazen and Finger, 1979); and (3) the fact that the simplest analysis of atomic motion relates vibrational frequencies to the displacement of the ion from its equilibrium distance: this distance should depend on how compressible the vibrating bond is, as well as the compressibility of the surrounding, but not necessarily participating, bonds. Another missing factor is the relative bond strength within the vibrating radical compared to that of the bonds from the radical to other ions in the structure, and the mass of the ions that the radical is bonded to. For example, bending motions and the rotation of the anions in B_{1g} will be at lower frequencies if heavy cations surround the O atoms of the XO_6 octahedron than if light ones are there. Such damping, in essence, is due to the

[1] A copy of Appendix Figures 6–9 may be ordered as Document AM-90-443 from the Business Office, Mineralogical Society of America, 1130 Seventeenth Street NW, Suite 330, Washington, DC 20036, U.S.A. Please remit $5.00 in advance for the microfiche.

TABLE 2. Comparison of inactive modes

	A_{2g}			$B_{1u}(1)$			$B_{1u}(2)$		
	This work	*	**	This work	*	**	This work	*	**
SiO_2	700	—		610	—		200	—	
GeO_2	630	557		460	714		150	215	
TiO_2	573†	566		406‡	631		113‡	220	
RuO_2	590	—		—	—		—	—	
MgF_2	370	326	360	410	467	436	120	210	207
NiF_2	—	370	304	360	476	371	100	167	155
ZnF_2	320	375	284	285	437	329	90	146	122
CoF_2	—	356	293	330	460	374	95	162	142
SnO_2	570	520		400	677		120	165	
FeF_2	310	368	321	370	414	343	100	131	175
MnF_2	310	323	264	—	408	350	—	147	121

* Maroni (1988).
** Striefler and Barsch (1974).
† Katiyar and Kirshnan (1967).
‡ Traylor et al. (1971).

effective mass of the O atom being augmented by that of its neighboring atoms. Thus, in a solid, frequencies are primarily determined by properties of the first nearest neighbors, but modified by the presence of second nearest neighbors.

Prediction of inactive modes

The consistent patterns of mode frequencies with cell volume (in Fig. 2) and bond length (in Fig. 3) can be used to predict the three inactive modes from measured values for one compound. Of the rutile type structures, TiO_2 alone has been thoroughly studied by IR, Raman, and INS (inelastic neutron scattering) spectroscopies. Unfortunately, the A_{2g} mode was not observed in INS by Traylor et al. (1971). Two calculations for TiO_2 (Katiyar and Krishnan, 1967; Maroni, 1988) give reasonable positions relative to the other gerade modes and values within a few wavenumbers of each other (Figs. 2a and 3a, filled triangles), suggesting that using the calculated value of A_{2g} will yield reasonable estimates for the inactive modes of the other compounds.

Estimates of the three inactive modes of the other compounds were made by first scaling the TiO_2 frequencies according to the factor of $1/[(X - O)^{3/2}\text{mass}^{1/2}]$ as defined by Batsanov and Derbeneva (1969). For the oxides, the estimated A_{2g} modes fall, on average, halfway between the A_{1g} and E_g modes. The trend has a similar slope. This suggests that the force constant for the A_{2g} mode is lattice dependent and is proportional to the lattice constant, to a first approximation. For consistency, and to predict vibrational frequencies for the fluorides as well as the oxides, the estimated points were adjusted to make the trend for the inactive modes analogous to the observed trends for the active modes in plots both of frequency as a function of cell volume (Fig. 2a) and of frequency as a function of cation-anion bond length (Fig. 3a). A proportional relationship was not used because of the slight irregularities in the relationships of the Raman modes with cell volume or bond length; instead, the positions of the estimated A_{2g} modes were adjusted so that the appearance of the trend in Figures 2a and 3a resembles as much as possible the trends of the Raman modes. The values of A_{2g} for the large volume cells (compiled in Table 2) are within ± 50 cm^{-1} of their true values, as bracketed by E_g and A_{1g} values, whereas values of A_{2g} for the small-volume cells are expected to be within ± 100 cm^{-1} of their true values.

Trial values of the inactive nodes obtained from $1/[(X - O)^{3/2}\text{mass}^{1/2}]$ (Batsanov and Derbeneva, 1969) were adjusted slightly in order to fit the trends of Figures 2 and 3. Initial estimates of $B_{1u}(1)$ frequencies (not shown) fall slightly above $E_u(2)$ LO for the large-volume compounds and slightly below for the small-volume compounds, but above $E_u(2)$ TO for all compounds except stishovite, whereas the low B_{1u} modes are located considerably below the $E_u(1)$ TO. The relationship of A_{2u} with cell volume or bond length shows more scatter, but most of the higher B_{1u} frequencies are below the A_{2u} curve. Because SnO_2 frequencies are undoubtedly underestimated by this technique [values for B_{1u} calculated by Katiyar and Krishnan (1967) are considerably higher], and rotational modes are expected to occupy a flatter trend, $B_{1u}(1)$ values were adjusted slightly upward or downward to give the least number of crossovers with the trends of the IR modes with both cell volume and bond length (Figs. 2b,c and 3b,c). The $B_{1u}(2)$ positions were adjusted by approximately the same percentage as $B_{1u}(1)$, as well as being made to mimic the lowest frequency E_u trend. The resulting trend of the lower energy B_{1u} mode is very shallow and is nearly equal to that of the lowest energy Raman mode, B_{1g}. When the consistency of the trends is considered, the true values of the inactive $B_{1u}(2)$ modes should be at least within ± 50 cm^{-1} of the predictions, whereas the $B_{1u}(1)$ modes will be within ± 100 cm^{-1}. The larger uncertainty is less important because the lowest energy modes will affect the calculation of elasticity or heat capacity the least.

Our estimates of the two B_{1u} and A_{2g} modes were also included in plots of ν^2 as a function of the force constant divided by the reduced mass (Fig. 4 and Appendix Fig.

8[1]), the reduced mass (Appendix Fig. 7[1]), and the force constant (Appendix Figs. 6[1] and 9[1]). In all cases, the patterns seen for the inactive modes predicted as discussed above strongly resemble the patterns of the active modes with k′, or μ, or k′/μ. Because there is no clear gain by using force constants over cell volume in estimating the inactive modes, we feel that it is advantageous to use the simpler, more direct relationship with the structural parameters.

Comparison of estimated inactive frequencies with valance bond force field (VBFF) calculations

Our predictions of the A_{2g} inactive modes compare well with Maroni's (1988) VBFF results (Table 2). Values for A_{2g} modes of the oxides are about 50 cm^{-1} higher than Maroni's values, whereas those of fluorides tend to be an equal amount lower. Maroni's estimates may be more accurate for the oxides, which define a line for the frequency vs. cell volume for the Raman, but their values for the fluorides are inconsistent with the trends of the measured frequencies with cell volume. Note that the calculations fall within the stated uncertainty of our estimates ($\pm$50 cm^{-1}) in every case.

Our predictions of the $B_{1u}(2)$ mode are generally about 100 cm^{-1} lower than Maroni's (1988) calculations, whereas our predictions of $B_{1u}(1)$ are usually 70 cm^{-1} lower. Maroni's calculations for TiO_2 are 100–150 cm^{-1} higher than the measured values (Table 2), and his calculations of either B_{1u} mode are not consistent with the trends in the IR data.

Similar relationships hold between Streifler and Barsch's (1974) rigid-ion calculations of the inactive modes for fluorides in the rutile structure and our estimates (Table 2).

Generally, Raman species are more readily calculated than IR modes because of difficulty in replicating the polarizability of the ions. By analogy, the gerade inactive modes may also be more easily calculated than the ungerade inactive species. This proposal rationalizes the variation in accuracy in the VBFF and rigid-ion calculations. We suggest that our estimates of the B_{1u} modes are a closer representation of the true values. At the least, our method provides for uncertainties to be established for estimated or calculated frequencies.

Conclusions

Changes in the $E_u(2)$ TO and $E_u(3)$ LO components of Roessler and Albers (1972) are proposed for GeO_2 with the rutile structure by comparison of new thin-film data with previous contradictory reflectance data of Kahan et al. (1971) and Roessler and Albers (1972). The revised data are in good agreement with peak positions obtained for other compounds with the rutile structure, in that, like dependencies on cell volume, bond lengths, and cation masses were seen. For the Raman modes, oxide frequencies depend nearly linearly on cell volume or on metal-O bond lengths, with similar slopes for each mode. The fluorides have linear trends with the same slopes, which are offset to lower frequencies. Mass effects are negligible for the Raman modes, as predicted from factor-group analysis. For the IR modes, the trends deviate from linearity, both oxides and fluorides occupy the same trend, and the trends for the A_{2u} modes cross over those of some of the E_u modes.

From the nearly linear dependence of optical modes with cell volume, and from comparison to the INS measurement on TiO_2, estimates of the inactive bands were made for GeO_2, SiO_2, and other compounds. The consistency of the trends suggests uncertainties of the estimates to within 100 cm^{-1} and usually to within less than 30 cm^{-1}. Our estimates of the A_{2g} modes are within experimental uncertainty of Maroni's (1988) calculations. His B_{1u} predictions are not consistent with trends in the IR data with cell volume, nor with measured values for TiO_2, suggesting that our estimates of the inactive modes are probably closer to the actual values.

Batsanov and Derbeneva's (1969) formulas for force constants were tested for 11 compounds with the rutile structure. Trends of ν with k were found to be no better, and sometimes were more irregular than trends of frequency with cell volume. We inferred that the failure is related to the absence of three factors in the derivation of force constants: bond compressibility, relative bond strength (compared to that for the second nearest neighbor), and the mass of the second nearest neighbors. The role of bond compressibility in determining the value of the vibrational frequencies in solids is apparent in the consistent relationship between frequency and cell volume for rutile structure compounds.

Acknowledgments

The synthesis and IR experiments were performed at the Geophysical Laboratory. We thank B. Mysen for use of his facilities and help with synthesis. A.M.H. was supported by NSF grants EAR-8419984 and EAR-8816531. J.H. and J.M.C. were supported as ACS SEED fellows. Critical reviews by W. White (Pennsylvania State University) and two anonymous reviewers were very helpful.

References cited

Balkanski, M., Moch, P., and Parisot, G. (1966) Infrared lattice-vibration spectra in NiF_2, CoF_2, and FeF_2. Journal of Chemical Physics, 44, 940–944.

Barker, A.S. (1964) Transverse and longitudinal optic mode study in MgF_2 and ZnF_2. Physical Review, 136, A1290–A1295.

Batsanov, S.S., and Derbeneva, S.S. (1969) Effect of valency and coordination of atoms on position and form of infrared absorption bands in inorganic compounds. Journal of Structural Chemistry (USSR), 10, 510–515.

Berreman, R.G. (1963) Infrared absorption at longitudinal optic frequency in cubic crystal films. Physical Review, 130, 2193–2198.

Boyd, F.R., and England, J.L. (1960) Apparatus for phase-equilibrium measurements at pressure. Journal of Geophysical Research, 65, 741–765.

Brout, R. (1959) Sum rule for lattice vibrations in ionic crystals. Physical Review, 113, 43–44.

Dayal, B. (1950) The vibration spectrum of rutile. Proceedings of the Indian Academy of Science, A32, 304–312.

Eagles, D.M. (1964) Infrared spectrum of rutile TiO_2. Journal of Physics and Chemistry of Solids, 25, 1243.

Hara, Y., and Nicol, M. (1979) Raman spectra and structure of rutile at high pressure. Physica Status Solidi, B94, 317–322.

Hazen, R.M., and Finger, L.W. (1979) Bulk modulus-volume relationship for cation-anion polyhedra. Journal of Geophysical Research, 84, 6723–6728.

Hemley, R.J. (1987) Pressure dependence of Raman spectra of SiO_2 polymorphs: α-quartz, coesite, and stishovite. In M.H. Manghani and Y. Syono, Eds., High pressure research in mineral physics, p. 347–360. Terra Scientific Publishing Company, Tokyo.

Hemley, R.J., Mao, H.K., and Chao, E.C.T. (1986) Raman spectrum of natural and synthetic stishovite. Physics and Chemistry of Minerals, 13, 285–290.

Hill, R.J., Newton, M.D., and Gibbs, G.V. (1983) A chemical study of stishovite. Journal of Solid State Chemistry, 47, 185–200.

Hofmeister, A.M., Xu, J., Mao, H.-K., Bell, P.M., and Hoering, T.C. (1989) Thermodynamics of Fe-Mg olivines at mangle pressures: Mid- and far-infrared spectroscopy at high pressure. American Mineralogist, 74, 281–306.

Hofmeister, A.M., Xu, J., and Akimoto, S. (1990a) Infrared spectroscopy of natural and synthetic stishovite. American Mineralogist, 75, 951–955.

Hofmeister, A.M., Chopelas, A., and Hemley, R.J. (1990b) Vibrational spectroscopy of end-member silicate garnets. Physics and Chemistry of Minerals, in press.

Huang, Y.S., and Pollak, F.H. (1982) Raman investigation of rutile RuO_2. Solid State Communications, 43, 921–924.

Kahan, A., Goodrum, J.W., Singh, R.S., and Mitra, S.S. (1971) Polarized reflectivity spectra of tetragonal GeO_2. Journal of Applied Physics, 42, 4444–4446.

Katiyar, R.S., and Krishnan, R.S. (1967) The vibrational spectrum of rutile. Physics Letters, 25A, 525–526.

Katiyar, R.S., Dawson, P., Hargreave, M.M., and Wilkinson, G.R. (1971) Dynamics of the rutile structure III. Lattice dynamics, infrared and Raman spectra of SnO_2. Journal of Physics C: Solid State Physics, 1971, 2421–2431.

Little, E.J., and Jones, M.M. (1960) A complete table of electronegativities. Journal of Chemical Education, 37, 231–245.

Mammone, J.F., Sharma, S.K., and Nicol, M. (1980) Raman study of rutile (TiO_2) at high-pressures. Solid State Communications, 34, 799–802.

Maroni, V.A. (1988) Valance force field treatment of the rutile structure at zero-wave vector. Journal of the Physics and Chemistry of Solids, 49, 307–313.

Mitra, S.S., and Marshall, R. (1964) Trends in the characteristic phonon frequencies of the NaCl-, diamond-, zinc-blende-, and wurtzite-type crystals, Journal of Chemical Physics, 41, 3158–3164.

Nicol, M., and Fong, M.Y. (1971) Raman spectra and polymorphism of titanium dioxide at high pressures. Journal of Chemical Physics, 54, 3167–3170.

Peercy, P.S., and Morosin, B. (1973) Pressure and temperature dependences of Raman-active phonons in SnO_2. Physical Review, B7, 2779–2786.

Porto, S.P.S., Fleury, P.A., and Damen, T.C. (1967) Raman spectra of TiO_2, MgF_2, ZnF_2, FeF_2, and MnF_2. Physical Review B, 154, 522–526.

Roessler, D.M., and Albers, W.A.J. (1972) Infrared reflectance of single crystal tetragonal GeO_2. Journal of the Physics and Chemistry of Solids, 33, 293–296.

Samara, G.A., and Peercy, P.S. (1973) Pressure and temperature dependencies of the static dielectric constants and Raman spectra of TiO_2 (rutile). Physical Review, B7, 1131–1148.

Scott, J.F., and Porto, S.P.S. (1967) Longitudinal and transverse optical lattice vibrations in quartz. Physical Review, 161, 903–910.

Sharma, S.K., Virgo, D., and Kushiro, I. (1979) Relationship between density, viscosity and structure of GeO_2 melts at low and high pressures. Journal of Non-Crystalline Solids, 33, 235–248.

Striefler, M.E., and Barsch, G.R. (1974) Optical mode gammas, pressure derivatives of elastic and dielectric constants, and stability of rutile-structure fluorides in the rigid ion approximation. Physica Status Solids, 64, 613–625.

Traylor, J.G., Smith, H.G., Nicklow, R.M., and Wilkinson, M.W. (1971) Lattice dynamics of rutile. Physical Review B, 10, 3457–3472.

Wyckoff, R.W.G. (1965) Crystal structures. Wiley, New York.

Manuscript received January 30, 1990
Manuscript accepted October 10, 1990